

Arthur von Hippel and Magnetism

John B. Goodenough

Abstract

This article examines the role that Arthur von Hippel played in magnetism work in the 1950s. Von Hippel understood that the ferrimagnetic insulators represented by the ferros spinels, magnetoplumbites, and ferrogarnets were critical for the high-frequency technology that was being developed after World War II. At the Laboratory for Insulation Research at MIT, he and his students concentrated on the response of these materials to electric and magnetic excitations over a wide frequency range that extended, with gaps, from dc to the ultraviolet. For magnetic studies, he used microwave frequencies to obtain resonance and relaxation data that could be interpreted because the magnetic spins are relatively loosely coupled to their surroundings. He supplemented these resonance studies with classical magnetometer, transport, and x-ray diffraction measurements on single-crystal samples in order to obtain fundamental information that would aid in the design of materials for technical applications.

Keywords: Arthur von Hippel, magnetism.

Introduction

During World War II, Arthur von Hippel established the Laboratory for Insulation Research at the Massachusetts Institute of Technology, where he performed his pioneering work on BaTiO_3 and other ferroelectrics. During that same period in Europe, J.L. Snoek and collaborators at the Philips Research Laboratories in Eindhoven, L. Néel with E.F. Bertaut and R. Pauthenet at the Institut Fourier in Grenoble, and C. Guillaud in Paris were quietly working on the ferros spinels MFe_2O_4 , where M is a divalent cation. Trivalent cations or $\text{M(IV)} + \text{M(II)}$ pairs were also substituted for Fe(III) . Many of these spinels were ferrimagnetic insulators of interest for high-frequency applications such as microwave devices, magnetostrictive transducers, and magnetic memory cores. It was therefore natural that the Laboratory for Insulation Research under von Hippel should shift some activity from ferroelectric to ferromagnetic oxides in the 1950s. During this period, the advent of nuclear reactors, which can provide a beam of neutrons, made possible neutron diffraction and therefore the direct determination of atomic magnetic order below the Curie temperature T_C , a development that would transform the study of magnetic materials. Moreover, the discovery of the hexagonal magneto-

plumbites ($x\text{BaO} \cdot y\text{Fe}_2\text{O}_3 \cdot z\text{MO}$) exhibiting a large magnetocrystalline anisotropy useful for hard (permanent) magnets and the low-loss ferrogarnets $\text{R}_3\text{Fe}_5\text{O}_{12}$ (R = rare earth or yttrium) added to the intense international activity in this field, a field that brought together engineers, physicists, and chemists/ceramists to understand better how to design materials that would enable a variety of new technologies. In this way, the field proved an incubator for the development of a cadre of scientists who would help to create the field of materials science and engineering that we know today.

The $\text{A[B}_2\text{]O}_4$ spinel structure is illustrated in Figure 1; it contains tetrahedral A sites and octahedral B sites in a close-packed oxide-ion array. The ferros spinels generally have collinear spins at the cations; the A-site and B-site spins are coupled antiparallel to one another, but the magnitudes of the magnetizations generated by the two sites are not equal, which gives a net ferrimagnetic moment $M = |M_B - M_A|$. A long-range magnetic-ordering temperature $T_C > 300$ K makes the ferros spinels useful in room-temperature applications.

In 1952, I joined a group at the MIT Lincoln Laboratory charged with developing a ceramic ferros spinel with a square B–H

hysteresis loop and a read–rewrite switching cycle under $6 \mu\text{s}$ for the random-access memory invented by Jay Forrester. Our success in this endeavor proved an important stepping stone for the development of the digital computer. Arthur von Hippel followed our work with enthusiasm; he was a most gracious link to the MIT campus.

Magnetite: The Verwey Transition

At the Laboratory for Insulation Research (LIR), von Hippel had decided to begin a series of fundamental studies on the ferros spinels with single crystals of what chemically appears to be the simplest of the family, Fe_3O_4 , but which, as will be discussed, has proven to be the most difficult to fully understand even though it had been used as far back as the ancient Greeks as a compass needle for navigation. In von Hippel's laboratory, Smiltens and Fryklund¹ had, by 1950, grown the first single crystals of stoichiometric magnetite, Fe_3O_4 . At the time, this feat required a sound knowledge of the oxygen equilibrium as a function of temperature. Smiltens' crystals were used by many of von Hippel's students and postdoctoral fellows to study the insulator–metal transition found near the Verwey temperature $T_V \approx 120$ K (see Figure 2, from Miles, Westphal, and von Hippel²). The transition was first noted by Millar³ in 1929 with a specific-heat measurement, but it is now commonly known as the Verwey transition; it occurs well below $T_C = 858$ K.

In 1950, most physicists were still enamored of the point-charge model for

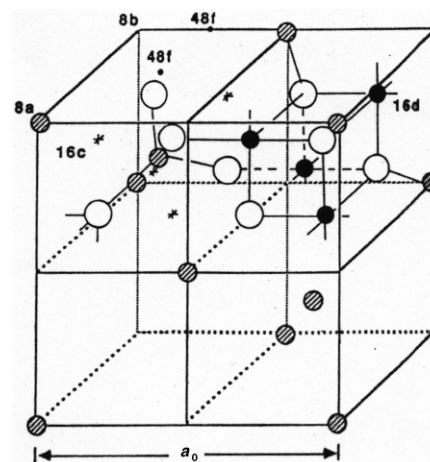


Figure 1. Two quadrants of the cubic $\text{A[B}_2\text{]O}_4$ spinel structure: A cations at 8a (hatched circles), B cations at 16d (solid circles), and oxygen at 48f (white circles).

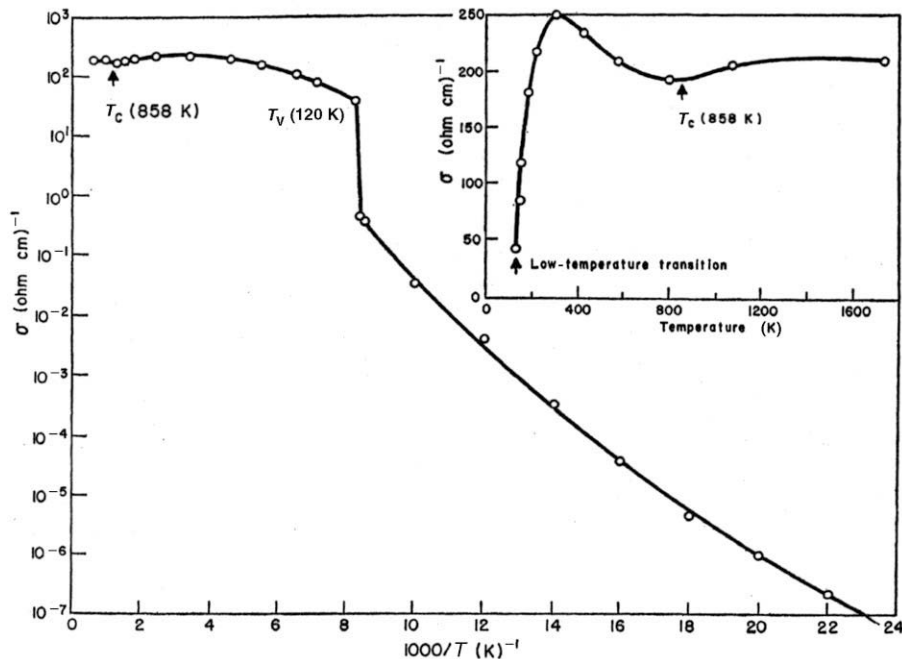


Figure 2. Temperature dependence of the dc conductivity of a magnetic single crystal. (After Reference 2).

ionic crystals, and all the 3d electrons of the ferrosinels, including the minority-spin electrons at the Fe^{2+} ions of Fe_3O_4 , were assumed to be localized. Therefore, the good room-temperature conductivity of Fe_3O_4 led Verwey⁴ to conclude that Fe_3O_4 must be an inverse spinel, that is, have the cation distribution $\text{Fe}^{3+}[\text{Fe}^{2+}\text{Fe}^{3+}]\text{O}_4$, which would allow electrons to hop between crystallographically equivalent sites. On the basis of a change from axial to cubic symmetry at T_V , Verwey further postulated a low-temperature ordering of the Fe^{3+} and Fe^{2+} ions onto alternate [100] and [010] rows of octahedral-site iron atoms. This model predicts orthorhombic symmetry for the low-temperature phase. It was this model that von Hippel's group set out to verify experimentally.

In 1951, Tombs and Rooksby⁵ reported that Fe_3O_4 is rhombohedral below T_V , in apparent contradiction of the Verwey prediction. However, in von Hippel's laboratory, Abrahams and Calhoun⁶ concluded from their x-ray diffraction data that the symmetry is orthorhombic or lower, and Bickford⁷ found deformations consistent with orthorhombic symmetry by using strain-gauge measurements on a Smilten single crystal that had been made single-domain below T_V by applying a uniaxial pressure along a [110] direction and cooling though T_V in the presence of a strong magnetic field applied along the c -axis. Hamilton,⁸ another von Hippel student,

performed a neutron diffraction study on a Smilten magnetite crystal at the Brookhaven National Laboratory to provide an apparent confirmation of orthorhombic symmetry below T_V , the Néel collinear ferrimagnetic spin configuration, and an easy magnetization axis along the cubic [001] axis lying close to the direction of a magnetic field applied during cooling; below T_V , that axis becomes the orthorhombic c -axis. With independent measurements, Bickford⁹ and Calhoun¹⁰ had already established the finding that below T_V , the [001] axis becomes the orthorhombic c -axis, which was first brought partially to light in 1932 by Li.¹¹

As a result of these studies, it was believed at the time that the Verwey model gave a correct description of Fe_3O_4 . However, in 1970 Hargrove and Kündig¹² published Mössbauer data showing an octahedral-site valence at room-temperature corresponding to $\text{Fe}^{2.5+}$; the conductive electrons were thus shown to hop from site to site in a time $\tau_h < 10^{-8}$ s. Moreover, below T_V , five peaks in the spectra could be distinguished, one for the A-site Fe^{3+} ions and four for the B-site ions. This result and early resistivity data of Calhoun⁹ together with Hall effect¹³ and thermoelectric power¹⁴ data suggested to Cullen and Callen¹⁵ that an itinerant (nonlocalized) electron model should be used for the minority spin electrons on the octahedral-site

iron ions; the majority spin electrons are clearly localized.

It now appears that the minority spin electrons are small polarons (i.e., dressed in a local lattice distortion) in the paramagnetic phase as a result of spin-disorder scattering, but they become increasingly delocalized on lowering the temperature below T_C as the octahedral-site spins become more ordered. For example, Figure 3 shows that the phonon contribution to the thermal conductivity is suppressed in the range $T_V < T < 300$ K, but is restored below T_V ;¹⁶ this result is consistent with vibronic Fe-Fe bonding with orbital fluctuations above T_V and orbital ordering with or without charge ordering below T_V . However, whether there is any charge ordering below T_V remained a matter of controversy until the complexity of the low-temperature structure could be clarified. Recent resonant x-ray scattering¹⁷ has confirmed the monoclinic Cc space group deduced by Iizumi et al.¹⁸ and Zuo et al.¹⁹ and has shown that all the octahedral-site Fe atoms have the same charge in the low-temperature phase. Therefore, Subías et al.¹⁷ have attributed the structural distortion to strong electron-phonon interactions. This result implies an orbital ordering that orders the Fe-Fe bonding between octahedral-site cations. A bond ordering that retains sharing of the minority spin electrons by more than one Fe atom is compatible with ferromagnetic Fe-Fe interactions on the octahedral-site array.

Magnetocrystalline Anisotropy of Magnetite

The availability of a Smilten¹ single crystal of Fe_3O_4 allowed Bickford⁹ in 1950 to study its magnetocrystalline anisotropy and g -factor (gyromagnetic ratio) by microwave resonance absorption. In a crystal of cubic symmetry, the anisotropy energy of the magnetization \mathbf{M} can be expressed as

$$E_a = K_0 + K_1(\alpha_1^2\alpha_2^2 + \alpha_2^2\alpha_3^2 + \alpha_3^2\alpha_1^2) + K_2(\alpha_1^2\alpha_2^2\alpha_3^2)\alpha \dots, \quad (1)$$

where K_0 , K_1 , and K_2 are constants and α_1 , α_2 , and α_3 are the direction cosines of \mathbf{M} with respect to the crystal axes. Landau and Lifshitz²⁰ had pointed out that this anisotropy leads to an effective magnetic field $H_{\text{eff}} \sim (K_1/\mu_0 M_s)$ for a single-domain single crystal if only the first-order term in Equation 1 is retained. Kittel²¹ derived an expression for the resonance frequency ω_0 of the precession of the magnetization about an applied magnetic field for an ellipsoidal crystal with crystallographic

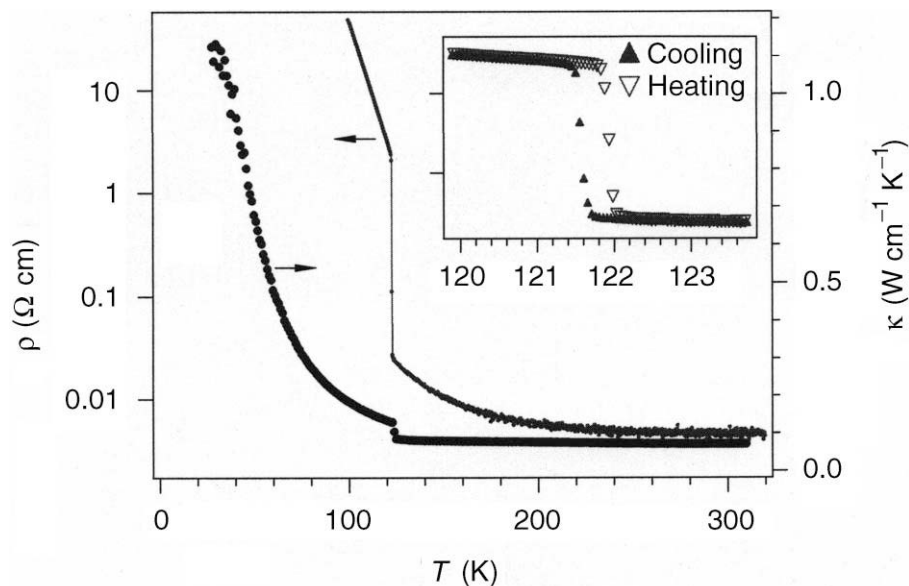


Figure 3. Temperature dependence of the resistivity $\rho(T)$ and thermal conductivity $\kappa(T)$ of a magnetite single crystal. Inset: thermal hysteresis of the thermal conductivity at T_V . (After Reference 16).

axes x , y , z along the principal axes of the ellipsoid:

$$\omega_0 = \gamma\mu_0[H_z + (N_y + N_y^e - N_z)M_z]^{1/2} [H_x + (N_x + N_x^e - N_z)M_z]^{1/2}, \quad (2)$$

where $\gamma = ge/2m$ is the gyromagnetic ratio (e is the charge of the electron and m is the mass of the electron); H_z is a static magnetic field applied along the z -axis; M_z is the component of \mathbf{M} along the z -axis; N_x , N_y , and N_z are the demagnetizing factors; and the extra contributions to N_x and N_y from the magnetocrystalline anisotropy of Equation 1 are

$$\begin{aligned} \mu_0 N_x^e &= (2K_1/M_z^2) \cos 4\theta \\ \mu_0 N_y^e &= (K_1/2M_z^2)(1 + \cos 4\theta), \end{aligned} \quad (3)$$

where θ is the angle between \mathbf{M} and a [100] direction in the (001) plane.

Corresponding expressions were derived for the (110) plane. In order to determine the two unknowns, g and K_1 , two measurements were made, one with the applied field parallel to the [100] axis and the other with it parallel to the [110] axis for an ellipsoid cut from the (100) crystal plane. For ellipsoids cut from the (110) crystal planes, the magnetic field was applied parallel to the [100] and [111] directions. The resonance induction $B_z = \mu_0 H_z$ is lowest in any crystal plane if it is near the direction of easy magnetization; it is highest near the direction of most difficult magnetization. From these measurements,

Bickford was able to show that K_1 changed sign on cooling, due to a change from a [110] to a [100] easy axis; the crystal was magnetically isotropic at 130 K, some 10 K above T_V . Below T_V , the cubic [100] axis nearest to the applied field became the easy [001] axis of the low-temperature phase. Bickford also found that the spectroscopic splitting factor decreases from $g = 2.12$ at room temperature to $g = 2.05$ at 130 K, which is close to the spin-only value $g = 2.0$. Thus, the orbital contribu-

Arthur von Hippel
understood the importance
of making a systematic
study with a wide range of
experimental techniques on
well-defined single crystals.

tion was shown to be significantly smaller than expected for an orbitally disordered, localized minority spin electron at Fe^{2+} ions just above T_V . However, an orbital ordering by the trigonal component of the crystalline field at an octahedral site of the spinel structure could be assumed responsible for quenching of the orbital angular momentum.

Domenicali²² developed a pendulum magnetometer in von Hippel's laboratory for the purpose of making magnetization

studies on the ferros spinels. Arthur von Hippel understood the importance of making a systematic study with a wide range of experimental techniques on well-defined single crystals. In addition to x-ray diffraction, ferromagnetic resonance, transport measurements, and magnetometer studies, his group used dielectric spectroscopy and developed a vibrating-coil magnetometer;²³ an upgraded version of the vibrating-coil magnetometer was used at the MIT Lincoln Laboratory for the measurement of magnetic properties under hydrostatic pressure.²⁴

Calhoun¹⁰ used the pendulum magnetometer to make torque measurements of the magnetocrystalline anisotropy of a Smiltens¹ single crystal. He also monitored the switching of the magnetization direction in the (110) plane on heating after cooling in a field of 10 kOe at angles of 0° , 25° , and 40° to [001] to establish that the c -axis of the low-temperature phase is oriented along the cubic [100] axis nearest the direction of the magnetizing field if the crystal is cooled in a magnetic field. Calhoun also measured the magnetic-field strength required to switch the c -axis below T_V from a cubic [100] to a cubic [010] axis. With the assumption that the switching requires a reordering of the Fe^{2+} and Fe^{3+} ions in the Verwey model by a cooperative electron transfer, Calhoun deduced an activation energy $U = 0.033$ eV for the electron exchange. He also noted that the electronic reordering gave rise to significant dimensional changes. Some type of electron reordering below T_V is made evident by this experiment and later studies by others on low-temperature reordering in a magnetic field by light excitation. If there is no charge ordering, a reordering of the Fe-Fe bonding responsible for the crystalline distortion must be taking place.

Cobalt-Substituted Magnetite

Substitution of Co^{2+} for Fe^{2+} in the spinel $\text{Fe}[\text{Fe}_{2-x}\text{Co}_x]\text{O}_4$ was known to impart a large magnetocrystalline anisotropy and magnetostriction that increased monotonically with x ; the large magnetostriction would be used in magnetic transducers. In 1953, Calhoun²⁵ and Bickford et al.²⁶ initiated a study of the effect of the magnetostriction imparted by Co on the permeability of magnetite. The changes with magnetic annealing on the magnetocrystalline anisotropy of Co-substituted magnetite were studied by Penoyer and Bickford²⁷ on Smiltens¹ single crystals.

Jahn and Teller had pointed out that if a localized-electron configuration at a molecule has an orbital degeneracy, the degeneracy can be removed by a lowering of the

site symmetry that orders the electron(s) among the orbitals. In a solid, a local site distortion costs an elastic strain energy, and this elastic energy is minimized by a cooperative orbital ordering at the ions having an orbital degeneracy. In an octahedral B site of a ferromagnetic spinel, the fivefold-degenerate d orbitals are split by the cubic crystalline field into twofold-degenerate σ -bonding e orbitals and threefold-degenerate π -bonding t orbitals. The concept of cooperative orbital ordering of twofold-degenerate σ -bonding e orbitals was only introduced in 1955 to account for the cubic to tetragonal ($c/a > 1$) transition in spinels containing octahedral-site Mn(II) and/or Cu(II) in excess of a critical concentration.²⁸ This concept had not yet been extended to ordering of threefold-degenerate, π -bonding t^4 or t^5 configurations. Only after 1957 was it appreciated that a collinear ordering of the octahedral-site spins below T_C in a ferrimagnetic ferromagnetic spinel would, through spin-orbit coupling, result in a cooperative orbital ordering of a t^5 configuration that enhanced the orbital angular momentum even where the concentration of Co^{2+} ions is small.²⁹⁻³¹ The trigonal crystal field at an octahedral site of the spinel structure stabilizes an orbital ordering that suppresses the orbital angular momentum at an Fe^{2+} ion, so the Co^{2+} ion is unique in its ability to impart a giant magnetostriction and magnetocrystalline anisotropy to a ferromagnetic spinel. Moreover, in 1955 few, if any, were aware of the distinction between *exchange striction*, which reflects the magnetic order, and *magnetostriction*, which reflects the crystallographic direction of the spin.

The initial permeability versus temperature curve of magnetite exhibits a sharp maximum at the magnetic isotropic temperature $T_{is} = 130$ K, where the easy magnetization axis changes. It was known that substitution of Co for Fe causes the maximum in the permeability to increase. Bickford et al.²⁶ used strain gauges to measure, from 120 K to room temperature, the magnetostriction coefficients of a series of Co-substituted magnetite single crystals. From the structural changes that occur on crossing T_{is} , which were amplified by the Co substitutions, they were able to demonstrate that the maximum in the initial permeability tracks T_{is} and that T_{is} increases nearly linearly by 140°C/mol% Co. A further deduction to be drawn from this experiment is that each Co^{2+} ion exerts an independent magnetocrystalline anisotropy energy favoring spin alignment along a [100] axis as a result of long-range cooperativity through spin-orbit coupling.

Penoyer and Bickford²⁷ investigated the variation under a magnetic anneal of the

magnetocrystalline anisotropy of Co-substituted magnetite; they annealed a Smilten single crystal at 375°C in a magnetic field of 10 kOe oriented at an angle θ_a from a cubic [001] axis in the (100) and (110) planes and from $[\bar{1}10]$ in the (111) plane. They used torque measurements made with a torque magnetometer at the IBM Research Center³² to obtain an anisotropy energy

$$W_A = K_1(\alpha_1^2\alpha_2^2 + \alpha_2^2\alpha_3^2 + \alpha_3^2\alpha_1^2) + W_U, \quad (4)$$

where the uniaxial component induced by the magnetic anneal was

$$W_U = -F\sum_i\alpha_i^2\beta_i^2 - G\sum_{i>j}\alpha_i\alpha_j\beta_i\beta_j. \quad (5)$$

The F and G are constants, and α_i and β_i are the direction cosines of the magnetization during the torque measurement and during the annealing process, respectively. Their data showed that the coefficients F and G of Equation 5 vary quadratically and linearly, respectively, with the Co concentration x in $\text{Fe}[\text{Fe}_{2-x}\text{Co}_x]\text{O}_4$. This finding enabled them to rule out theories that depended on cation diffusion and to introduce the concept that the individual Co^{2+} ion sites have, below T_C , a symmetry axis that responds to a magnetic anneal by a cooperative reorientation of their axes to align themselves with the magnetizing field. This experiment showed a clear connection between a giant magnetostriction and magnetocrystalline anisotropy introduced by individual octahedral-site Co^{2+} ions.

Site-Preference Energies

Another topic of general interest was the origin of the preferences of ions for the octahedral versus the tetrahedral sites in a spinel. From electrostatic arguments, the cation of larger charge should be stabilized on the octahedral sites of a spinel. The quadrivalent ions are found on the octahedral sites, but V(V) occupies a tetrahedral site in $\text{V}[\text{LiCo}]\text{O}_4$ and $\text{V}[\text{LiNi}]\text{O}_4$ because of its strong tetrahedral-site preference. Of more immediate interest were the II–III spinels. Electrostatic arguments predicted normal spinels, $A^{2+}[\text{B}_2^{3+}]\text{O}_4$, but magnetite proved to be an inverse spinel, $\text{Fe}^{3+}[\text{Fe}^{2+}\text{Fe}^{3+}]\text{O}_4$. From the crystal-field splitting, it was apparent that the transition-metal cations with d^3 , low-spin d^6 , and high-spin d^8 configurations have a strong octahedral-site preference and that the larger crystal-field splitting at an octahedral site could give high-spin Fe^{2+} and Co^{2+} ions a small octahedral-site prefer-

ence. However, the observation that $\text{Mg}_x\text{Fe}_{1-x}[\text{Mg}_{1-x}\text{Fe}_{1+x}]\text{O}_4$ is a mixed spinel was surprising, since $\text{Zn}[\text{Fe}_2]\text{O}_4$ and $\text{Cd}[\text{Fe}_2]\text{O}_4$ are normal spinels. This observation implies that cations with d^{10} and high-spin d^5 configurations have a stronger tetrahedral-site preference than the more basic Mg^{2+} ions and therefore that M–O covalence plays an important role; the point-charge model does not give an adequate description of the oxides.

At the LIR, Epstein and Frackiewicz³² measured as a function of temperature the fraction x of Mg^{2+} ions on the tetrahedral sites of $\text{Mg}_x\text{Fe}_{1-x}[\text{Mg}_{1-x}\text{Fe}_{1+x}]\text{O}_4$. They did this by studying the cation distribution at room temperature after the samples had been quenched from different annealing temperatures. They also obtained kinetic data by measuring the time for the cation distribution to reach equilibrium at 600°C after quenching from different temperatures.

The “After-Effect” in Iron Garnets

The oxygen stoichiometric polycrystalline iron garnets $\text{Y}_3\text{Fe}_5\text{O}_{12}$ and $\text{Lu}_3\text{Fe}_5\text{O}_{12}$ show normal behavior, but those that are only slightly reduced (or oxidized) exhibit several unusual properties: a uniaxial magnetocrystalline anisotropy that is induced by annealing in a magnetic field,³⁴ a domain-wall relaxation,^{35,36} and B–H hysteresis loops that vary with the frequency of the applied magnetic field at liquid-nitrogen temperature.³⁷ Epstein et al.³⁶ found a uniaxial anisotropy energy as high as 450 J/m² in a polycrystalline sample of $\text{Lu}_3\text{Fe}_5\text{O}_{12}$ that had been cooled in a magnetic field to 78 K. In a subsequent study of the “dynamic squareness” of the B–H hysteresis loop in polycrystalline garnets, Lovell and Epstein³⁷ were able to conclude that all of these unusual properties could be explained by the Néel³⁸ diffusion “after-effect” model in which the magnetic field induces a preferred ordering of the Fe^{2+} ions with respect to the oxygen vacancy (or Fe^{4+} with respect to a cation vacancy) that introduced them; electron (or hole) trapping occurs at lower temperatures. Any change in the orientation of the local magnetization, and specifically the reorientation that occurs within a moving domain wall, forces an irreversible redistribution of the mobile charge carriers. Since this reorientation extracts energy that is dissipated to the lattice, the moving domain walls behave as though they were retarded by a viscous drag. Janak³⁹ added to this damping the intrinsic damping that is always present because of the spin–spin relaxation processes that occur within a moving domain wall. The Janak model of the damped re-

sponse of a 180° domain wall to a step or a ramped magnetic-field excitation was able to account for the following unusual properties that had been observed:

1. The B–H hysteresis loop has a dynamic squareness at 78 K at a nearly fixed maximum field strength.
2. There is a large increase with frequency in the coercivity below the maximum field strength for the loop squareness.
3. Under ramp excitation, the domain walls move stably until a critical field strength is reached. If the allowed excursion of the wall has not been reached at the critical field strength, the wall jumps to a new position to give a square-loop behavior.
4. When a step excitation is applied, the wall does not reach its terminal velocity immediately because of its inertia. It exhibits a highly damped motion below its critical velocity and, provided its terminal velocity is not much above its critical velocity, increases rather slowly toward the critical velocity. Therefore, induced voltages by the changing magnetic flux $d\phi/dt$ (where t is time) are small until instability occurs.

Summary

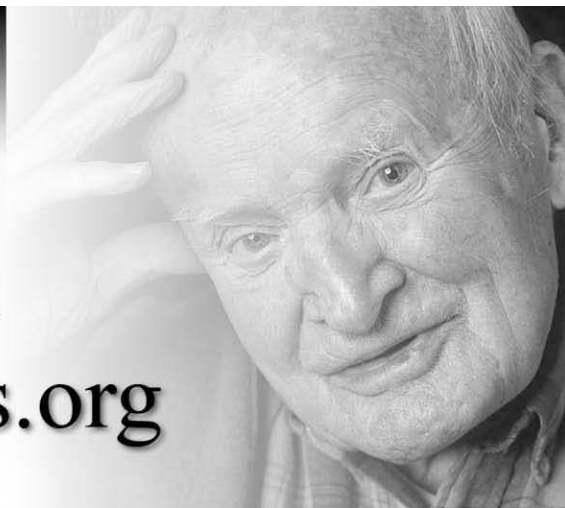
Arthur von Hippel understood that the ferrimagnetic insulators represented by the ferros spinels, magnetoplumbites, and ferrogarnets were critical for the high-frequency technology that was being developed post–World War II. At the Laboratory for Insulation Research at MIT, he and his students concentrated on the response of these materials to electric and magnetic excitations over a wide frequency range that extended, with gaps, from dc to the ultraviolet. For magnetic studies, he used microwave frequencies to obtain resonance and relaxation data that could be interpreted because the magnetic

spins are relatively loosely coupled to their surroundings. He supplemented these resonance studies with classical magnetometer, transport, and x-ray diffraction measurements on single-crystal samples in order to obtain fundamental information that would aid in the design of materials for technical applications. In the process, he trained a cadre of students without taking undue credit to himself and became a father of modern materials science. The Materials Research Society has correctly recognized this role by naming its highest honor the Von Hippel Award.

References

1. J. Smiltens and D.H. Fryklund, Laboratory of Insulation Research, Massachusetts Institute of Technology, 1950; J. Smiltens, *J. Chem. Phys.* **20** (1952) p. 990.
2. P.A. Miles, W.B. Westphal, and A. von Hippel, *Revs. Mod. Phys.* **29** (1957) p. 279.
3. R.W. Millar, *J. Am. Chem. Soc.* **51** (1929) p. 215.
4. E.J. Verwey, *Nature* **144** (1939) p. 337; E.J.W. Verwey and P.W. Haayman, *Physica* **8** (1941) p. 979; E.J.W. Verwey, P.W. Haayman, and F.C. Romeijn, *J. Chem. Phys.* **15** (1947) p. 181.
5. N.C. Tombs and H.P. Rooksby, *Acta Cryst.* **4** (1951) p. 474.
6. S.C. Abrahams and B.A. Calhoun, *Acta Cryst.* **6** (1953) p. 105; S.C. Abrahams and B.A. Calhoun, *Acta Cryst.* **8** (1955) p. 257.
7. L.R. Bickford Jr., *Revs. Mod. Phys.* **25** (1953) p. 75.
8. W.C. Hamilton, *Phys. Rev.* **110** (1958) p. 1050.
9. L.R. Bickford Jr., *Phys. Rev.* **78** (1950) p. 449.
10. B.A. Calhoun, *Phys. Rev.* **94** (1954) p. 1577.
11. C.H. Li, *Phys. Rev.* **40** (1932) p. 1002.
12. R.S. Hargrove and W. Kündig, *Solid State Commun.* **8** (1970) p. 303.
13. W.J. Siemons, *IBM J. Res. Develop.* **14** (1970) p. 245.
14. C. Constantin and M. Rosenberg, *Solid State Commun.* **10** (1972) p. 675.
15. J.R. Cullen and E. Callen, *Phys. Rev. Lett.* **26** (1971) p. 236; J.R. Cullen and E. Callen, *Phys.*

- Rev. B* **7** (1973) p. 397.
16. J.-S. Zhou, unpublished.
17. G. Subías, J. García, J. Blasco, M.G. Proietti, H. Renevier, and M.C. Sanchez, *Phys. Rev. Lett.* **93** 156408 (2004).
18. M. Iizumi, T.F. Koetzle, G. Shirane, S. Chikazumi, M. Matsui, and S. Todo, *Acta Cryst. B* **38** (1982) p. 2121.
19. J.M. Zuo, C.H. Spence, and W. Petuskey, *Phys. Rev. B* **42** (1990) p. 8451.
20. L. Landau and E. Lifshitz, *Physik. Z. Sowjetunion* **8** (1931) p. 135.
21. C. Kittel, *Phys. Rev.* **73** (1948) p. 155; C. Kittel, *Phys. Rev.* **76** (1949) p. 743.
22. C.A. Domenicali, *Rev. Sci. Instr.* **21** (1950) p. 327.
23. D.O. Smith, *Rev. Sci. Instr.* **27** (1956) p. 261.
24. N. Menyuk, J.A. Kafalas, K. Dwight, and J.B. Goodenough, *Phys. Rev.* **177** (1969) p. 942.
25. B.A. Calhoun, *Technical Report of Laboratory for Insulation Research* (Massachusetts Institute of Technology, Cambridge, Mass., July 1953) unpublished.
26. L.R. Bickford Jr., J. Pappis, and J.L. Stull, *Phys. Rev.* **99** (1955) p. 1210.
27. R.F. Penoyer and L.R. Bickford Jr., *Phys. Rev.* **108** (1957) p. 271.
28. J.B. Goodenough and A.L. Loeb, *Phys. Rev.* **98** (1955) p. 391.
29. J. Kanamori, *Progr. Theoretical Physics (Kyoto)* **17** (1957) p. 197.
30. J.C. Slonzewski, *Phys. Rev.* **110** (1958) p. 1341.
31. J.B. Goodenough, *Magnetism and the Chemical Bond* (Wiley Interscience, New York, 1963).
32. R.F. Penoyer, *Rev. Sci. Instr.* **30** (1959) p. 711.
33. D.J. Epstein and B. Frackiewicz, *J. Appl. Phys.* **29** (1958) p. 376.
34. B.A. Calhoun, *J. Appl. Phys.* **30** (1959) p. 2935.
35. D.J. Epstein and B. Frackiewicz, *J. Appl. Phys.* **30** (1959) p. 2955.
36. D.J. Epstein, B. Frackiewicz, and R.P. Hunt, *J. Appl. Phys.* **32** (1961) p. 2705.
37. B.W. Lovell and D.J. Epstein, *J. Appl. Phys.* **34** (part 2) (1963) p. 1115.
38. L. Néel, *J. Phys. Radium* **13** (1952) p. 246.
39. J.F. Janak, *J. Appl. Phys.* **34** (1963) p. 1119. □



MRS celebrates the life and times of Arthur von Hippel

<http://vonhippel.mrs.org>